AIAA Aviation
13-17 June 2016, Washington, D.C.
46th AIAA Fluid Dynamics Conference

CrossMark
click for updates

Computation of Turbulent Flow in a Rotating Pipe using the Elliptic Blending Reynolds Stress Model

Neil Ashton *
Oxford e-Research Centre, University of Oxford, UK

Michael Stoellinger †
Department of Mechanical Engineering, University of Wyoming

The flow through a axially rotating pipe is examined using the open-source code OpenFOAM for both standard eddy-viscosity models (Spalart-Allmaras & $k-\omega$ SST) and a low-Reynolds number Elliptic Blending Reynolds Stress Model with a homogenous turbulent dissipation rate equation. Corrections to the length-scale determining equation for rotation, based upon the work of Hellsten et al. (1998), are evaluated for both the SST and EB-RSM models. It is shown that for models with or without a rotation correction, the EB-RSM offered improved results over the SST model, better capturing the level of turbulence suppression and the parabolic circumferential velocity profile. A clear improvement to both the SST and EB-RSM models is observed when a Richardson correction is applied to the length-scale determining equations, resulting in much closer agreement to the experimental data. The results for the EB-RSM with this correction are in good agreement with previous studies and further improvements to the turbulent diffusion model would likely improve the correlation to the experiment even further. The performance of the SST model is better than expected although the reliance of both models on the Richardson correction suggests further work is needed to thoroughly assess the formulation of such corrections for a wider range of flows.

Downloaded by Neil Ashton on July 27, 2016 | http://arc.aiaa.org | DOI: 10.2514/6.2016-3943

I. Introduction

Computational Fluid Dynamics (CFD) has grown to become an essential component of the engineering design process. With computational resources becoming cheaper and more powerful, its use has allowed a greater understanding of the behaviour of fluid flows and has become a crucial tool to assess new designs and concepts. This increased computational resource also means that for many problems grid convergence is now becoming possible with Reynolds-Averaged Navier-Stokes (RANS) approaches. Arguably therefore it is the turbulence modelling approach that is key to achieving greater accuracy and correlation to experimental data. Whilst the availability and power of computational resources has grown, they are not yet powerful enough and readily available to use methods such as Large Eddy Simulation (LES) for routine use by aerospace engineers. Thus in the short to medium term, the majority of engineering simulations will still be conducted using RANS [1] even if they do not provide the predictive capability of higher-fidelity methods [2].

Turbulent swirling and rotating flows are common to many engineering applications, from the vortices produced by airplanes and racing cars to the flow inside pipes and ducts. Correctly predicting these type of flows is crucial to obtaining accurate results from CFD simulations of complete complex systems such as an entire aircraft or a Formula 1 car. In order to assess the capability of RANS models to capture these types of flows it is helpful to use simple test cases that isolate the important flow physics in a simulation that can be grid converged and run using readily available computational resources. A popular test-case within the aerospace and motorsport community is the NACA0012 wing-tip [3], which has been subject to a number of CFD studies [4–6]. The major conclusions from these studies was that standard linear eddy-viscosity models e.g Spalart-Allmaras, $k-\omega$ SST, $k-\varepsilon$ could not accurately capture the resulting wing-tip vortex, typically over-predicting the turbulent viscosity and thus damping out the vortex too early. Modifications to these standard models for rotation showed improvements but could not match the predictive capability of Reynolds-Stress models which were able to capture the anisotropy of the flow to a greater extent [6]. However, none of these studies reported grid convergence and work by the author (unpublished as yet) found grid convergence still lacking even at more than 200 million cells for a 2^{nd} order finite-volume code using cartesian-prismatic unstructured grids. Without grid convergence it is not possible to truly focus on the turbulence modelling as the primary source of

*Senior Researcher, Oxford e-Research Centre, University of Oxford, AIAA Senior Member.
†Assistant Professor, Department of Mechanical Engineering, Dept. 3295, AIAA Member

Copyright © 2016 by Neil Ashton, Michael Stoellinger. Published by the American Institute of Aeronautics and Astronautics, Inc., with permission.

error. In addition such large meshes make turbulence model development extremely expensive. For this reason it is desirable to find a test case that contains the physics related to rotation and curvature but which can easily reach grid convergence. One such case is a axially rotating pipe, which is the focus of this work.

II. Rotating Pipe

Despite its geometric simplicity this case displays complex physics that makes it an ideal test for turbulence models. We consider the setup that is used in Zaets et al.[7] ; a stationary pipe of diameter, $D = 0.06$m and length, $100D$, which leads into a rotating pipe section of the same diameter and length 25D. We also consider the setup of Nishibori et al.[8] where the rotating pipe section is extended to $200D$. The previous experimental and computational studies[9–12] have shown two distinct regions in the rotating pipe section. In the first $20 - 40D$ an increase in the vorticity due to the rotation of the pipe causes a region of strong turbulence suppression[7,10], where all components of the Reynolds stresses and turbulent dissipation rate decrease and the azimuthal velocity reaches a parabolic limit (in contrast to a laminar flow which would reaches a linear solid-body rotation profile). Following this until $\approx 170D$ a saturation region exists where the turbulent statistics and mean flow reach a constant value.

From a computational standpoint the majority of studies have shown that this is a difficult flow for RANS models to capture[13]. Standard eddy-viscosity models have shown largely poor results, with Torri et al.[12] demonstrating an inability of the $k - \varepsilon$ model to predict the effects of rotation unless corrections (using the Richardson correction[14]) are included in the ε equation. However only limited results were presented so it is difficult to conclude the true performance of eddy-viscosity models. The conclusions of Torri et al. are however in contrast with the work of Hirai et al.[15] and Wallin et al.[16] who concluded that the $k - \varepsilon$ fails (with or without the Richardson correction for Hirai et al.). Speziale et al.[13] (also discussed in Jakirlic et al.[9]) demonstrated the theoretical inability of standard two-equation models to account for rotation, however this appeared to be for a flow subject to a rotating reference frame and the additional complexity of the fully-developed inlet flow means that in practice the performance of these models may partly reproduce the rotation-effects because of the influence of the changing pressure and azimuthal velocity[9].

The majority of other studies focused on Reynolds Stress Models, where a strong sensitivity to both the form of the pressure-strain model[11], turbulent diffusion model[10] and the length-scale providing equation[10] were observed. In Poroseva et al.[11] it was found that the use of the commonly used Daly-Harlow[17] model for the turbulent diffusion could not accurately capture the turbulent suppression. A new turbulent diffusion model[10] solving a transport equation for the triple moment correlations was found to offer improved results (albeit at the expense of numerical stability). Later work by Poroseva et al.[11] also noted a sensitivity to the form of the pressure-strain model with the Q structured model providing the most accurate results. The majority of these CFD studies used some form of correction for rotation in the length-scale providing equation, typically based upon the Richardson correction[10]. Most authors noted that worse results were obtained without such a correction, however exactly how 'quiet' these corrections are in other flow configurations (or whether these corrections are only implemented for particular flows) is a major disadvantage for general purpose CFD applications.

III. Turbulence models

Three turbulence models are evaluated; Spalart-Allarmas (SA)[18], $k - \omega$ SST[19] and a low-Reynolds Reynolds-Stress model, the EB-RSM-ε_H[20]. The SA and SST models were implemented in OpenFOAM v2.3.0 according to their published form (which is described on the NASA Turbulence Modelling Resource website [‡] and in Gomez et al.[21]). The default versions of the SA and SST models in OpenFOAM v2.3 do not match the original published forms of the models thus a modified version was implemented based upon the original publications. In addition, for both the SST and EB-RSM a form of the Richardson correction is evaluated based upon the form proposed by Hellsten et al.[22], as shown in Equation 1 [§].

$$Ri = \frac{|\Omega_{ij}|}{|S_{ij}|}\left(\frac{|\Omega_{ij}|}{|S_{ij}|} - 1\right) \tag{1}$$

Which is used in the respective length-scale providing equations as a function to effectively reduce the β or $C\varepsilon_2$

[‡]http://turbmodels.larc.nasa.gov

[§]We note that the SA model has various rotation and curvature corrections, which will be the focus of future investigation

Downloaded by Neil Ashton on July 27, 2016 | http://arc.aiaa.org | DOI: 10.2514/6.2016-3943

coefficient in areas of rotation:

$$F_{rc} = \frac{1}{1 + C_{rc}Ri} \tag{2}$$

C_{rc} is a tuneable coefficient, which is set to $C_{rc} = 1.4$ for the SST model (the original value of 3.6 in [22] was found to be overly suppressive of turbulence, as also suggested by Mani et al. [23]) and $C_{rc} = 0.8$ for the EB-RSM. It should be noted that the tuning of such values for C_{rc} is undesirable and is likely to be case-specific thus we use this correction with some caution. Simulations using this correction as referred to as SST-RC-HELLSTEN and EBRSM-RC-HELLSTEN.

What follows is a description of the EB-RSM ε_h model [20] referred to in this paper as the EB-RSM model.

A. Elliptic Blending RSM model

We consider incompressible flows for which the Reynolds averaged Navier-Stokes equations are given by

$$\frac{\partial \overline{u}_i}{\partial x_j} = 0 \tag{3}$$

and,

$$\frac{\partial \overline{u}_i}{\partial t} + \overline{u}_j \frac{\partial \overline{u}_i}{\partial x_j} = -\frac{\partial \overline{p}}{\partial x_i} + \nu \frac{\partial^2 \overline{u}_i}{\partial x_j \partial x_j} - \frac{\partial \tau_{ij}}{\partial x_j}, \tag{4}$$

where $\overline{u}_i$ denotes the Reynolds averaged velocity and $\tau_{ij} = \overline{u'_i u'_j}$ denotes the Reynolds stress tensor. The RSMeb model is a modification of the standard Elliptic Blending model by Manceau [24]. The main novelty is given by the use of the homogeneous dissipation rate ε^h as the scale providing equation. The modeled transport equation for the Reynolds stress tensor is given by

$$\frac{\partial \tau_{ij}}{\partial t} + \overline{u}_j \frac{\partial \tau_{ij}}{\partial x_j} = P_{ij} + \Phi^*_{ij} - \varepsilon^h_{ij} + \frac{\partial}{\partial x_k}\left[\left(0.5\nu\delta_{kl} + C_k \frac{k}{\varepsilon^h}\tau_{kl}\right)\frac{\partial \tau_{ij}}{\partial x_l}\right], \tag{5}$$

where P_{ij} is the production, Φ^*_{ij} is the pressure redistribution term, ε^h_{ij} is the homogeneous dissipation rate tensor [25] and the last term represents molecular diffusion and turbulent transport according to the Daly-Harlow model [17] with $C_k = 0.21$. The factor of one half for the molecular diffusion term results from the use of the homogeneous dissipation rate [25]

$$\varepsilon^h = \varepsilon - 0.5\nu \frac{\partial^2 k}{\partial x_l x_l}, \tag{6}$$

where k is the turbulent kinetic energy $k = \tau_{ll}/2$. The production term is given by

$$P_{ij} = -\tau_{ik}\frac{\partial \overline{u}_j}{\partial x_k} - \tau_{jk}\frac{\partial \overline{u}_i}{\partial x_k}. \tag{7}$$

In the EB model the redistribution term is given by a "linear blending" of a near wall model Φ^w_{ij} and a homogeneous model Φ^h_{ij} that is appropriate away from the wall

$$\Phi^*_{ij} = (1 - f_\alpha)\Phi^w_{ij} + f_\alpha \Phi^h_{ij}, \tag{8}$$

where $f_\alpha = \alpha^3$ is the blending function which is based on the variable α that defines the "closeness" to a solid wall and that satisfies an elliptic equation [24]:

$$\alpha - L_d^2 \nabla^2 \alpha = 1. \tag{9}$$

The boundary conditions are such that at solid walls $\alpha = 0$ and in the free stream $\alpha = 1$. The Durbin-limited [26] length scale L_d is given by

$$L_d = max\left(C_L \frac{k^{3/2}}{\varepsilon^h}, C_\eta \frac{\nu^{3/4}}{(\varepsilon^h)^{1/4}}\right), \tag{10}$$

Downloaded by Neil Ashton on July 27, 2016 | http://arc.aiaa.org | DOI: 10.2514/6.2016-3943

with constants $C_L = 0.13$ and $C_\eta = 10$. The dissipation rate tensor is also given by a blending between the near wall anisotropic form and the common isotropic form far away from the wall[24,25]

$$\varepsilon^h_{ij} = (1 - f_\alpha)\frac{\tau_{ij}}{k}\varepsilon^h + f_\alpha \frac{2}{3}\varepsilon^h \delta_{ij}. \tag{11}$$

The homogeneous part of the redistribution term is modeled according to the SSG model[27]

$$\begin{aligned}\Phi^h_{ij} = &-\left(C_{g1} + C^*_{g1}\frac{P}{\varepsilon^h}\right)\varepsilon^h a_{ij} + C_{g2}\left(a_{ik}a_{kj} - \frac{1}{3}a_{kl}a_{kl}\delta_{ij}\right) + \left(C_{g3} - C^*_{g3}\sqrt{a_{kl}a_{kl}}\right)kS_{ij} \\ &+ C_{g4}k\left(a_{ik}S_{jk} + a_{jk}S_{ik} - \frac{2}{3}a_{lm}S_{lm}\delta_{ij}\right) + C_{g5}k\left(a_{ik}\Omega_{jk} + a_{jk}\Omega_{ik}\right),\end{aligned} \tag{12}$$

where $P = P_{kk}/2$ is the production of turbulent kinetic energy, $a_{ij} = \tau_{ij}/k - 2/3\delta_{ij}$ is the anisotropy tensor, $S_{ij} = 1/2\left(\frac{\partial \overline{u}_i}{\partial x_j} + \frac{\partial \overline{u}_j}{\partial x_i}\right)$ is the rate-of-strain tensor, and $\Omega_{ij} = 1/2\left(\frac{\partial \overline{u}_i}{\partial x_j} - \frac{\partial \overline{u}_j}{\partial x_i}\right)$ is the rate-of-rotation tensor. The model coefficients are $C_{g1} = 1.7$, $C^*_{g1} = 0.9$, $C_{g2} = 1.05$, $C_{g3} = 0.8$, $C^*_{g3} = 0.65$, $C_{g4} = 0.625$, $C_{g5} = 0.2$.

The near wall form of the redistribution model was derived in[28] such that the correct asymptotic behavior is obtained

$$\Phi^w_{ij} = -5\frac{\varepsilon^h}{k}\left(\tau_{ik}n_j n_k + \tau_{jk}n_i n_k - \frac{1}{2}\tau_{kl}n_k n_l\left(n_i n_j + \delta_{ij}\right)\right), \tag{13}$$

where the wall normal vector $\vec{n}$ is also obtained from the elliptic variable α by

$$\vec{n} = \frac{\nabla\alpha}{\|\nabla\alpha\|}. \tag{14}$$

The closure of the dissipation rate equation follows the proposal of Jakirlić and Hanjalić[25] but with a simplified term for the viscous production:

$$\frac{\partial \varepsilon^h}{\partial t} + \overline{u}_j\frac{\partial \varepsilon^h}{\partial x_j} = C_{\varepsilon 1}P\frac{\varepsilon^h}{k} - C_{\varepsilon 2}F_{rc}f_\varepsilon\frac{\tilde{\varepsilon}^h\varepsilon^h}{k} + E_\varepsilon + \frac{\partial}{\partial x_k}\left[\left(0.5\nu\delta_{kl} + C_\varepsilon\frac{k}{\varepsilon^h}\tau_{kl}\right)\frac{\partial \varepsilon^h}{\partial x_l}\right], \tag{15}$$

with

$$E_\varepsilon = 2C_{\varepsilon 3}\nu\frac{k^2}{\varepsilon^h}(1-\alpha)\left(\frac{\partial^2\overline{u}_i}{\partial x_k \partial x_k}\right)^2, \tag{16}$$

and

$$\tilde{\varepsilon}^h = \varepsilon^h - \nu\left(\frac{\partial\sqrt{k}}{\partial n}\right)^2. \tag{17}$$

F_{rc} is the Richardson correction as described in Equation 2. The $(1-\alpha)$ term in (16) ensures that the viscous production term is only active near the wall. The function f_ε is modified from a Re_t dependent formulation[25] to be a function of the elliptic near wall variable α and is given by

$$f_\varepsilon = 1 - \frac{C_{\varepsilon 2} - C_{\varepsilon 1}}{C_{\varepsilon 2}}\exp\left[-(7\alpha)^5\right]. \tag{18}$$

The model coefficients are given by:

$$C_{\varepsilon 1} = 1.44, \quad C_{\varepsilon 2} = 1.82, \quad C_{\varepsilon 3} = 0.005, \quad C_\varepsilon = 0.18. \tag{19}$$

The boundary conditions at the wall are

$$\overline{u}_i = 0, \quad \tau_{ij} = 0, \quad \varepsilon^h = \nu\frac{k}{y_1^2}, \quad \alpha = 0, \tag{20}$$

where y_1 is the wall normal distance of the first cell center.

Downloaded by Neil Ashton on July 27, 2016 | http://arc.aiaa.org | DOI: 10.2514/6.2016-3943

The divergence of the Reynolds stress tensor in (4) is implemented through a deferred correction approach. The stress tensor is split into two contributions

$$\tau_{ij} = \tau_{ij}^{impl} + \tau_{ij}^{expl} = -\nu_t \left(\frac{\partial \overline{u}_i}{\partial x_j} + \frac{\partial \overline{u}_j}{\partial x_i} \right) + \tau_{ij}^{expl}, \tag{21}$$

and the linear eddy viscosity part is treated implicitly and the difference $\tau_{ij} - \tau_{ij}^{impl}$ is treated explicitly and lagged in time. The turbulent viscosity is calculated by

$$\nu_t = C_\mu \frac{k^2}{\varepsilon^h} \det\left(\frac{\tau_{ij}}{k}\right), \tag{22}$$

with $C_\mu = 0.28$. This expression for turbulent viscosity provides the correct near wall behaviour.

The Reynolds stress model based on the elliptic blending as described above does not depend on a geometrically defined wall distance and wall normal direction which makes it very well suited for complex wall bounded flows. The recent review paper of Manceau et al.[24] provides more details on the origin of the model and the various versions that have been developed since its inception.

Downloaded by Neil Ashton on July 27, 2016 | http://arc.aiaa.org | DOI: 10.2514/6.2016-3943

IV. Computational Setup

In this study we investigate the configuration studied experimentally in Zaets et al.[7]; a stationary pipe of diameter, $D = 0.06$m and length, $100D$, which leads into a rotating pipe section of the same diameter and length 25D. In this work we extend the rotating pipe to 200D to investigate the recovery of the flow further down the pipe as studied experimentally in Nishibori et al.[8]. Asymmetric conditions are assumed, where the inflow conditions are set to match the experimental conditions[7]; $Re_\tau = 875$ and $Re_m = 37000$ at $x/D = -200$. A pressure-outlet condition is imposed at the end of the rotating pipe section, $x/D = 200$. A no-slip condition is applied at the pipe wall in the stationary section and a velocity of $W = N \times U_0$ is applied to the wall in the rotating section.

Five successively finer grids were used to demonstrate grid convergence from 500×16 to 8000×256, each with $y^+ < 1$. It was found that grid convergence was reached by 4000×128 although further reductions of the mesh in the streamwise spacing could reduce the cell count.

All simulations were conducted in OpenFOAM using an incompressible steady-state solver based upon the SIMPLE pressure-velocity coupling method (simpleFoam). Second order accurate upwind schemes (linearUpwind) were used for spatial discretization for both the momentum and turbulent quantities.

V. Results

A. ZPG Flat Plate

To verify the implementation of the selected turbulence models in OpenFOAM, we assessed their performance on a number of test-cases from the NASA Turbulence Modelling Benchmark Group website [¶]. For brevity we only show the results for a zero-pressure gradient flat-plate, using a grid of 545x385 cells, where it can be seen that the SST and SA results from OpenFOAM (incompressible) agree within the expected range with the results from CFL3D (compressible). We also exploit the availability of recent DNS data[29] [‖] to examine the Reynolds stresses at $Re_\theta = 6500$. It can seen that the Reynolds stresses, and their anisotropy is much better captured by the EB-RSM, with the SST model under and over-predicting the streamwise and wall-normal components. The SST offers a better prediction of the streamwise velocity, however this may be due to the lack of tuning of the EB-RSM for high-Reynolds numbers flows. Close agreement with CFL3D/FUN3D was also reported for the 2D wall-mounted hump[30] and 2D bump-in-a-channel which gives confidence that these models have been properly implemented into OpenFOAM by the authors.

B. Rotating pipe

In the following figures we focus on radial profiles at $x/D = -10$ and $x/D = 25$ as well as profiles in the axial direction from $x/D = 0 - 25$ and $x/D = 0 - 200$. It can be seen from the experimental data in Figure 2 that the

[¶] http://turbmodels.larc.nasa.gov

[‖] http://torroja.dmt.upm.es/turbdata/blayers/high_re/

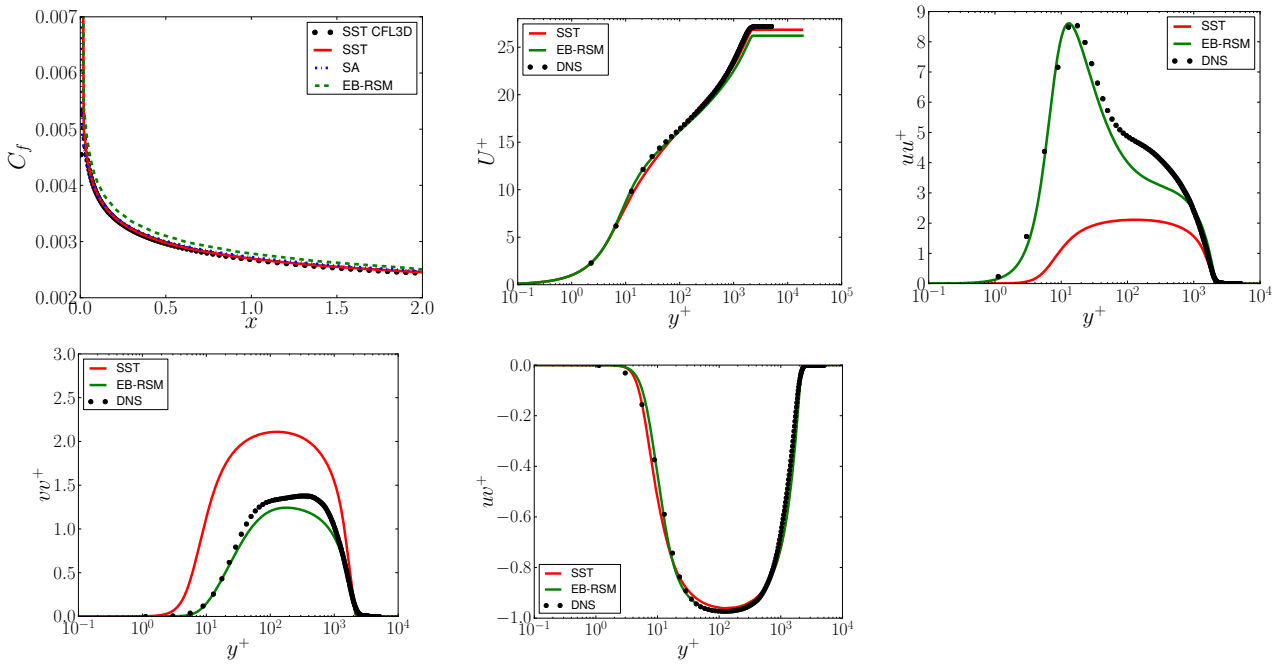

Figure 1. ZPG Flat Plate: (Left to Right), Skin-Friction Coefficient (C_f) Streamwise Velocity (U^+), Reynolds stresses (uu^+, vv^+& uv^+) for SA (C_f only), SST and EB-RSM, compared to DNS data[29] at $Re_\theta = 6500$

effect of rotation (at a moderate swirl rate of N=0.6) is an increase in the streamwise velocity in the centre of the pipe and a decrease near the wall. With increasing rotation rates this eventually moves toward a laminar profile[31] but not until $N > 2$. The azimuthal velocity profile in Figure 2 shows a parabolic profile at $N = 0.6$, rather than a linear profile which would be expected for a solid-body rotation e.g observed in a laminar flow[31]. We see in Figure 2 that the rotation causes a suppression of the Reynolds stresses which is often described as re-laminarization[31], although the profiles move towards a parabolic limit rather than a linear one which would be observed in a truly laminar flow[10].

In Figure 2 it can be seen that SA model fails to account for the rotation and predicts the opposite trend to the experiment, producing an increase in the turbulent shear-stress rather than a suppression. The model does not predict the correct parabolic circumferential velocity profile, showing a profile towards that of a laminar flow. This is likely due to the vorticity based production term of the SA model that under the action of the wall rotation increases vorticity and thus increases turbulence rather than suppressing it.

For the SST model, contrary to the analysis of Speziale et al.[13] the SST does not predict a linear-profile for the circumferential velocity although it is not able to agree with the experimental parabolic profile. Whilst the theoretical work of Speziale et al. is not necessarily wrong, the effect of a fully-developed inflow and the influence of a changing pressure and velocity field is likely to provide enough stimulus to account for some of the results. The SST model does show turbulence suppression but the amount is limited compared to the experiment. This is also true for the turbulent shear-stress and turbulent dissipation rate shown in Figure 3, where the correct trend is observed but the magnitude does not agree with the experimental values. In Figure 4 we see the level of turbulence suppression as measured by the damping coefficient, $Ku = < u'u' > (N > 0) / < u'u' > (N = 0)$. As expected the SST model underpredicts the level of suppression and also the anisotropic nature of this change. The same damping coefficient is displayed in the axial direction in Figure 5, where at both $r/R = 0$ and $r/R = 0.6$ the turbulence suppression is consistently under-predicted. Very similar results were obtained for the SST model in Olsen et al.[32] using OVERFLOW giving extra weight to the findings of this paper.

The results using the EB-RSM are within the expected range compared to the previous CFD studies which use the Daly-Harlow turbulent diffusion model[10] and no rotation correction in the ε equation. The correct parabolic profile for the circumferential velocity is obtained (Figure 2) and the turbulence suppression is also observed, although the level is under-predicted compared to the experiment. The turbulent kinetic energy is slightly over-predicted in both the stationary and rotating cases although it was observed in Kurbatskii et al.[10], that the use of a more sophisticated turbulent diffusion model reduced the level of k and the turbulent shear stress (Figure 3) at r/R 0.9. The streamwise

Downloaded by Neil Ashton on July 27, 2016 | http://arc.aiaa.org | DOI: 10.2514/6.2016-3943

velocity is slightly under-predicted compared to the experimental values although the trend is well captured. Compared to the SST model the reduction in the turbulent dissipation rate is well predicted by the EB-RSM for N=0.6, however the suppression in the Reynolds Stresses (as shown in Figure 4 and 5) is still under-predicted leading to a recovery in the turbulence levels beyond the stationary levels. This is agreement with the work of Kurbatskii et al.[10] and others who found that there was a particular sensitivity and link between the predicted turbulent suppression in the initial rotating section and the recovery further down the pipe.

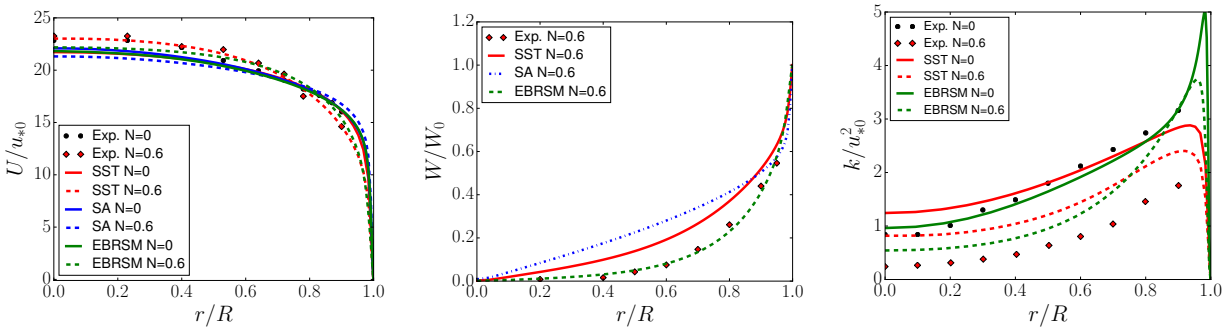

Figure 2. Rotating Pipe (N=0.6): (Left to Right), Streamwise Velocity (U/u_{*0}), Circumferential velocity W/W_0 and Turbulent Kinetic Energy (k/u_{*0}^2) for the SA (U and W), SST and EB-RSM, compared to experimental data of Zaets et al.[7].

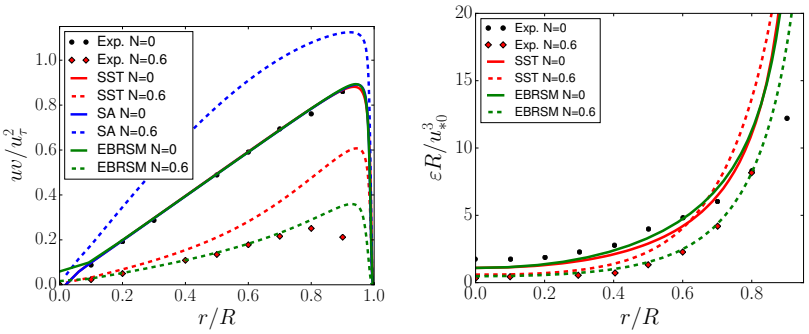

Figure 3. Rotating Pipe (N=0.6): (Left to Right), Reynolds Stress ($u'v'/u_{*0}^2$) and Turbulent Dissipation Rate ($\varepsilon R/u_{*0}^3$) for the SA ($u'v'$ *only*), SST and EB-RSM, compared to experimental data of Zaets et al.[7].

1. Rotation correction

As identified in Jakirlic et al.[9] a limiting factor in RSM models is the ε equation. There is no explicit term which can properly account for rotation due to the semi-empirical nature of its modelling. In the majority of previous CFD studies some form of correction was made to the length-scale determining equation[10–12] thus for both the SST and EB-RSM model we take the approach of Hellsten et al.[22], described in Equation 1. We use this formulation as it is both coordinate-invariant and does not use a turbulent time scale that may become unphysical in some parts of the flow[22]. As previously stated we use these corrections with some caution as their performance across a wide range of complex flows have not been established. For the single tuneable coefficient, C_{rc} we take the value of $C_{rc} = 1.4$ for the SST model, as the original coefficient of 3.6 was overly suppressive of the turbulence (as found in[23]). For the EB-RSM we use the same formulation for the Richardson correction although we use a coefficient of $C_{rc} = 0.8$. This coefficient was only assessed on this flow and therefore further tuning would be required to ensure it was suitable for as wide as range of flows as possible.

Figures 6 to 9 show the results for the SST and EB-RSM with and without the rotation correction. We see a clear improvement for both models, in particular for the turbulence suppression, where the damping of the Reynolds stresses are in much better agreement with the experimental data. The SST model is still unable to predict a parabolic circumferential velocity profile, which is most likely related to the Boussinesq assumption[13]. However whilst both models (in particular the EB-RSM) predict the suppression at $x/D = 25$ the agreement along the whole pipe is less

Downloaded by Neil Ashton on July 27, 2016 | http://arc.aiaa.org | DOI: 10.2514/6.2016-3943

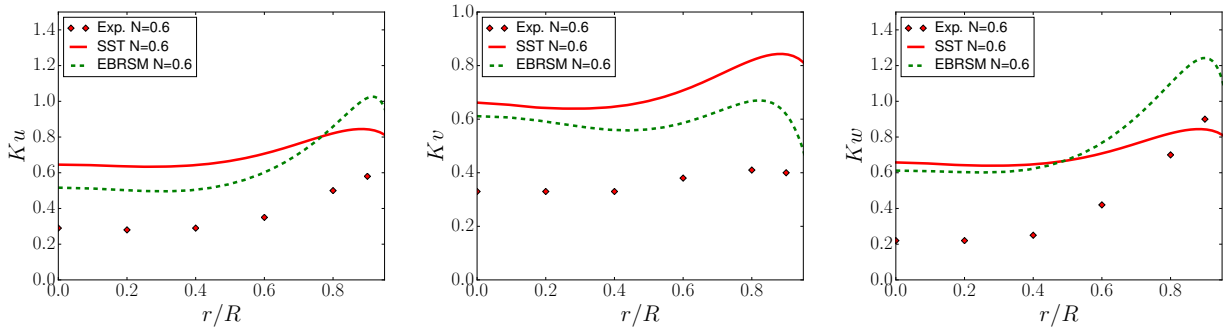

Figure 4. Rotating Pipe (N=0.6): (Left to Right), Damping coefficient $Ku =< u'u' > (N > 0)/ < u'u' > (N = 0)$ at $x/D = 25$, Damping coefficient $Kv =< v'v' > (N > 0)/ < v'v' > (N = 0)$ at $x/D = 25$ and Damping coefficient $Kw =< w'w' > (N > 0)/ < w'w' > (N = 0)$ at $x/D = 25$ for the SST and EB-RSM, compared to experimental data of Zaets et al.[7].

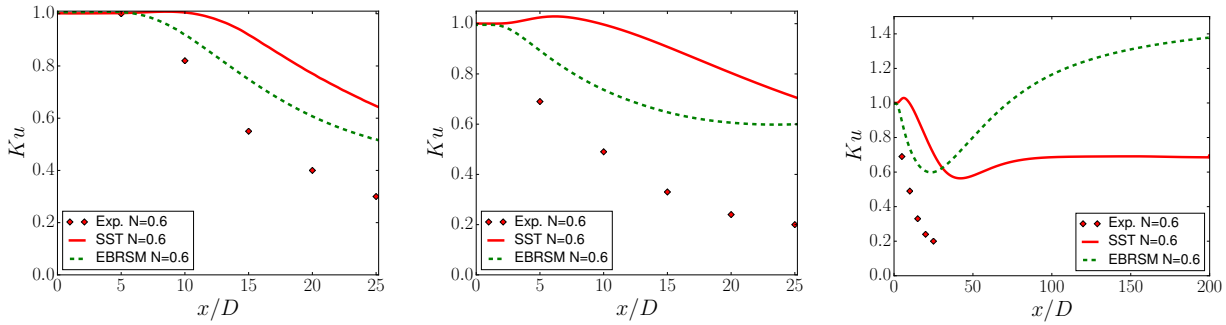

Figure 5. Rotating Pipe (N=0.6): (Left to Right), Damping coefficient Ku at $r/R = 0$, Damping coefficient Ku at $r/R = 0.6$ and Damping coefficient Ku at $r/R = 0.6$ (whole pipe length) for the SST and EB-RSM, compared to experimental data of Zaets et al.[7].

satisfactory. It can be seen in Figure 9 that both models under-predict the suppression at $r/R = 0.6$ but over-predict at $r/R = 0$. The lack of experimental data for the long-pipe configuration makes it hard to draw firm conclusions but work in Nishibori et al.[8] suggests a region of recovery after the initial suppression to a level below the stationary pipe values. Thus the models with the rotation correction term agree with this trend (as opposed to the EB-RSM without any correction) although the precise agreement is not possible to determine without further experimental or DNS data.

VI. Summary & Conclusions

The flow through an axially rotating pipe has been examined using the open-source code OpenFOAM for both standard eddy-viscosity models (SA & SST) and the Elliptic Blending Reynolds Stress Model with a homogenous turbulent dissipation rate equation. Corrections for rotation were applied to the length-scale determining equation of the SST and EB-RSM models based upon the work of Hellsten et al[22]. It was found that for models with or without the rotation correction the EB-RSM offered improved results over the SST model, better capturing the level of turbulence suppression and the parabolic circumferential velocity profile. There was however a clear improvement to both models when the Richardson correction was applied to the length-scale determining equations, resulting in much closer agreement to the experimental data. The results for the EB-RSM with the Richardson correction are in good agreement with previous studies and further improvements to the turbulent diffusion model would likely improve the correlation to the experiment even further. The performance of the SST model has been better than expected although the reliance of both models on semi-empirical corrections suggests further work is needed to thoroughly assess the formulation of such corrections for a wider range of flows. Further work is also needed to relate the conclusions of this flow to other rotating and vortex driven flows such as the NACA0012 wing-tip, to assess if conclusions from this test case can be related to more complex test cases.

Downloaded by Neil Ashton on July 27, 2016 | http://arc.aiaa.org | DOI: 10.2514/6.2016-3943

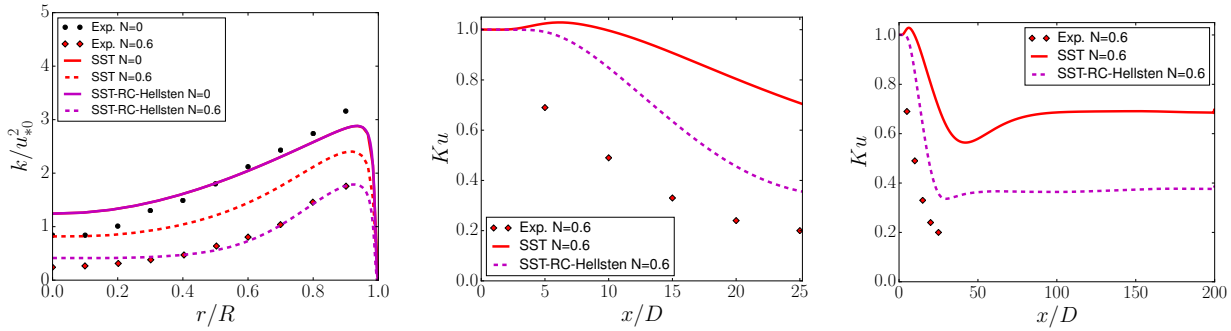

Figure 6. Rotating Pipe (N=0.6): (Left to Right), Turbulent Kinetic Energy (k/u_{*0}^2), Damping coefficient Ku at $r/R = 0.6$ and Damping coefficient Ku at $r/R = 0.6$ (whole pipe length) for the SST and SST-RC-HELLSTEN, compared to experimental data of Zaets et al.[7].

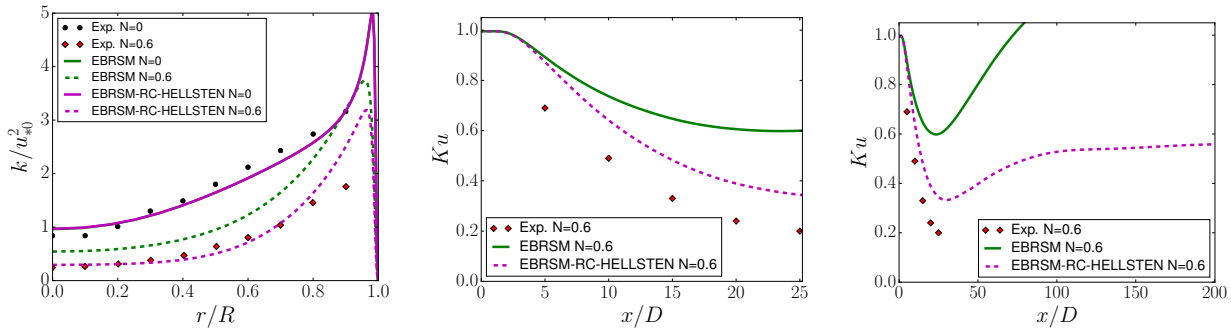

Figure 7. Rotating Pipe (N=0.6): (Left to Right), Turbulent Kinetic Energy (k/u_{*0}^2), Damping coefficient Ku at $r/R = 0.6$ and Damping coefficient Ku at $r/R = 0.6$ (whole pipe length) for the EB-RSM and EB-RSM-RC-HELLSTEN, compared to experimental data of Zaets et al.[7].

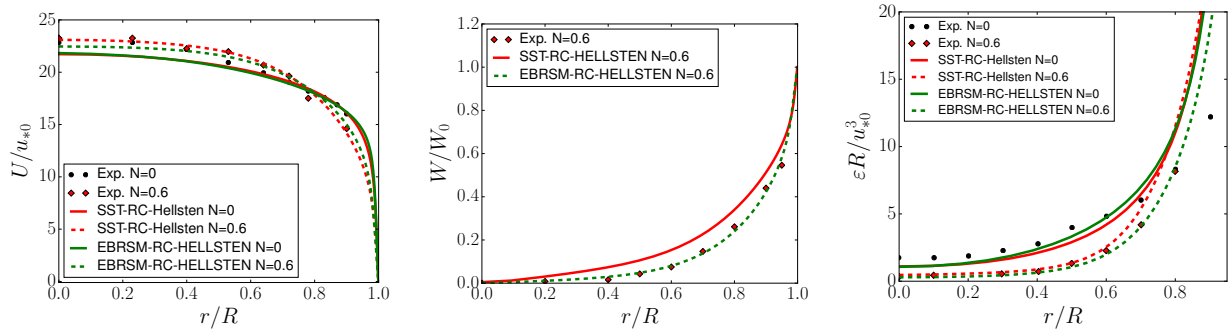

Figure 8. Rotating Pipe (N=0.6): (Left to Right), Streamwise Velocity (U/u_{*0}), Circumferential velocity W/W_0 and Turbulent Dissipation Rate ($\varepsilon R/u_{*0}^3$) for the SST-RC-HELLSTEN and EB-RSM-RC-HELLSTEN, compared to experimental data of Zaets et al.[7].

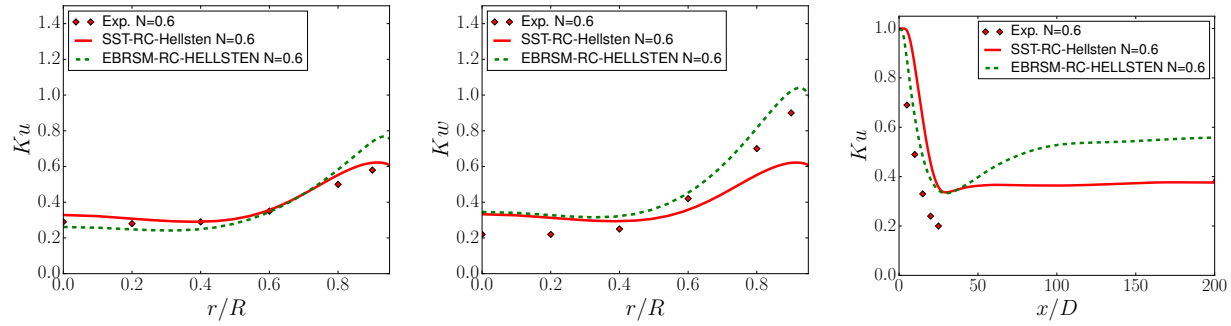

Figure 9. Rotating Pipe (N=0.6): (Left to Right), Damping coefficient Ku at $x/D = 25$, Damping coefficient Kw at $x/D = 25$ and Damping coefficient Ku at $r/R = 0.6$ for the SST-RC-HELLSTEN and EB-RSM-RC-HELLSTEN, compared to experimental data of Zaets et al.[7].

Downloaded by Neil Ashton on July 27, 2016 | http://arc.aiaa.org | DOI: 10.2514/6.2016-3943

VII. Acknowledgements

The authors would like to acknowledge the use of the University of Oxford Advanced Research Computing (ARC) facility in carrying out this work. http://dx.doi.org/10.5281/zenodo.22558. Special thanks to Michael Olsen (NASA Ames Research Centre) and Professor Svetlana Poroseva (University of New Mexico) for their helpful discussions on this work.

References

[1]P. R. Spalart and V. Venkatakrishnan, "On the role and challenges of CFD in the aerospace industry," *The Aeronautical Journal*, vol. 120, no. 1223, pp. 209–232, 2016. [Online]. Available: http://www.journals.cambridge.org/abstract{_}S000192401500010X

[2]N. Ashton and A. Revell, "Key factors in the use of DDES for the flow around a simplified car," *International Journal of Heat and Fluid Flow*, vol. 54, pp. 236–249, 2015. [Online]. Available: http://linkinghub.elsevier.com/retrieve/pii/S0142727X15000673

[3]J. S. Chow, D. Analyses, and P. Bradshaw, "Mean and Turbulence Measurements in the Near Field of a Wingtip Vortex," *AIAA Journal*, vol. 35, no. 10, pp. 1561–1567, 1997.

[4]T. J. Craft, A. V. Gerasimov, B. E. Launder, and C. M. E. Robinson, "A computational study of the near-field generation and decay of wingtip vortices," *International Journal of Heat and Fluid Flow*, vol. 27, no. 4, pp. 684–695, 2006.

[5]M. J. Churchfield and G. a. Blaisdell, "Reynolds Stress Relaxation Turbulence Modeling Applied to a Wingtip Vortex Flow," *AIAA Journal*, vol. 51, no. 11, pp. 2643–2655, nov 2013. [Online]. Available: http://arc.aiaa.org/doi/abs/10.2514/1.J052265

[6]S. Lardeau and R. Manceau, "Computations of complex flow configurations using a modified Elliptic-Blending Reynolds-Stress Model," in *ETMM10: 10th International ERCOFTAC Symposium on Engineering*, 2014.

[7]P. G. Zaets, A. F. Kurbatskii, A. T. Onufriev, S. V. Poroseva, N. A. Safarov, R. A. Safarov, and S. N. Yakovenko, "Experimental study and mathematical simulation of the characteristics of a turbulent flow in a straight circular pipe rotating about its longitudinal axis," *Journal of Applied Mechanics and Technical Physics*, vol. 39, no. 2, pp. 249–260, mar 1998. [Online]. Available: http://link.springer.com/10.1007/BF02468091

[8]K. NISHIBORI, K. KIKUYAMA, and M. MURAKAMI, "Laminarization of turbulent flow in the inlet region of an axially rotating pipe." *JSME international journal*, vol. 30, no. 260, pp. 255–262, 1987. [Online]. Available: http://joi.jlc.jst.go.jp/JST.Journalarchive/jsme1987/30.255?from=CrossRef

[9]S. Jakirlic, K. Hanjalic, and C. Tropea, "Modeling Rotating and Swirling Turbulent Flows: A Perpetual Challenge," *AIAA Journal*, vol. 40, no. 10, pp. 1984–1996, 2002. [Online]. Available: http://doi.aiaa.org/10.2514/2.1560

[10]A. F. Kurbatskii and S. V. Poroseva, "Modeling turbulent diffusion in a rotating cylindrical pipe flow," *International Journal of Heat and Fluid Flow*, vol. 20, pp. 341–348, 1999.

[11]S. V. Poroseva, S. C. Kassinos, C. a. Langer, and W. C. Reynolds, "Structure-based turbulence model: Application to a rotating pipe flow," *Physics of Fluids*, vol. 14, no. 4, pp. 1523–1532, 2002.

[12]S. Torii and W.-J. Yang, "Numerical prediction of fully developed turbulent swirling flows in an axially rotating pipe by means of a modified k-e turbulence model," *International Journal of Numerical Methods for Heat & Fluid Flow*, vol. 5, no. 2, pp. 175–183, 1995.

[13]C. G. Speziale, B. A. Younis, and S. A. Berger, "Analysis and modelling of turbulent flow in an axially rotating pipe," *Journal of Fluid Mechanics*, vol. 407, no. April 1999, pp. 1–26, 2000. [Online]. Available: http://www.scopus.com/inward/record.url?eid=2-s2.0-0033940035{&}partnerID=tZOtx3y1

[14]P. Bradshaw, D. H. Ferriss, and N. P. Atwell, "Calculation of boundary-layer development using the turbulent energy equation," *Journal of Fluid Mechanics*, vol. 28, no. September 1965, pp. 593–616, 1967.

[15]S. Hirai, T. Takahi, and M. Matsumoto, "Predictions of the laminarization phenomena in an axially rotating pipe flow," *Journal of Fluids Engineering*, vol. 4, 1987.

[16]S. Wallin and A. V. Johansson, "An explicit algebraic Reynolds stress model for incompressible and compressible turbulent flows," *Journal of Fluid Mechanics*, vol. 403, pp. 89–132, 2000.

[17]B. J. Daly and Harlow, "Transport equations in turbulence," *Phys. Fluids*, vol. 13, pp. 2634–2649, 1970.

[18]P. R. Spalart and S. R. Allmaras, "A one-equation turbulence model for aerodynamic flows," *La Recherche Aerospatiale*, vol. 1, pp. 5–21, 1994.

[19]F. R. Menter, "Two-Equation Eddy-Viscosity Turbulence Models for Engineering Applications," *AIAA*, vol. 32, no. 8, pp. 1598–1605, 1994.

[20]M. K. Stoellinger, R. Roy, and N. Ashton, "Application of an Elliptic Blending Reynolds Stress Model in Attached and Separated flows (Invited)," in *22nd AIAA Computational Fluid Dynamics Conference*, no. June. Reston, Virginia: American Institute of Aeronautics and Astronautics, jun 2015, pp. 1–12. [Online]. Available: http://arc.aiaa.org/doi/10.2514/6.2015-2926

[21]S. Gomez, B. J. Graves, and S. V. Poroseva, "On the Accuracy of RANS Simulations of 2D Boundary Layers with OpenFOAM," *AIAA Journal*, no. June, pp. 1–9, 2014.

[22]A. Hellsten, "Some Improvements in Menter's k-omega SST Turbulence Model," in *AIAA Paper 98-2554*, 1998, pp. 1–11.

[23]M. Mani, J. A. Ladd, and W. W. Bower, "Rotation and Curvature Correction Assessment for One-and Two-Equation Turbulence Models," *Journal of Aircraft*, vol. 41, no. 2, pp. 268–273, 2004.

[24]R. Manceau, "Recent progress in the development of the Elliptic Blending Reynolds-stress model," *International Journal of Heat and Fluid Flow*, vol. 51, pp. 195–220, 2015. [Online]. Available: http://linkinghub.elsevier.com/retrieve/pii/S0142727X14001179

[25]S. Jakirlic and K. Hanjalic, "A new approach to modelling near-wall turbulence energy and stress dissipation," *Journal of Fluid Mechanics*, vol. 539, pp. 139–166, 2002.

[26]P. Durbin, "Limiters and wall treatments in applied turbulence modeling," *Fluid Dynamics Research*, vol. 41, no. 1, p. 012203, feb 2009.

[27]C. G. Speziale, S. Sarkar, and T. B. Gatski, "Modelling the pressure strain correlation of turbulence: an invariant dynamical systems approach," *Journal of Fluid Mechanics*, vol. 227, pp. 245–272, 1991.

Downloaded by Neil Ashton on July 27, 2016 | http://arc.aiaa.org | DOI: 10.2514/6.2016-3943

[28]R. Manceau and K. Hanjalic, "Elliptic blending model: A new near-wall Reynolds-stress turbulence closure," *Physics of Fluids*, vol. 14, pp. 744–754, 2001.

[29]J. A. Sillero, J. Jiménez, and R. D. Moser, "Two-point statistics for turbulent boundary layers and channels at Reynolds numbers up to Re_{\theta} 2000," *Physics of Fluids*, vol. 26, no. 10, 2014.

[30]D. Greenblatt, K. B. Paschal, C. S. Yao, J. Harris, N. W. Schaeffler, and A. E. Washburn, "A separation control CFD validation test case, Part 1: baseline and steady suction," *AIAA paper 2004-2220*, 2004.

[31]L. Facciolo, N. Tillmark, A. Talamelli, and H. P. Alfredsson, "A study of swirling turbulent pipe and jet flows," *Physics of Fluids*, vol. 19, no. 3, 2007.

[32]M. E. Olsen, "Reynolds-stress and triple-product models applied to flows with rotation and curvature," in *46th AIAA Fluid Dynamics Conference*. Reston, Virginia: American Institute of Aeronautics and Astronautics, jun 2016. [Online]. Available: http://arc.aiaa.org/doi/10.2514/6.2016-3942

Downloaded by Neil Ashton on July 27, 2016 | http://arc.aiaa.org | DOI: 10.2514/6.2016-3943